

International Journal of Food Engineering

Volume 7, Issue 6

2011

Article 4

Low Temperature Drying With Air Dehumidified by Zeolite for Food Products: Energy Efficiency Aspect Analysis

Mohamad Djaeni, *Diponegoro University*

C. J. van Asselt, *Wageningen University*

P. V. Bartels, *Wageningen University*

J. P. M. Sanders, *Wageningen University*

Gerrit van Straten, *Wageningen University*

Anton J. van Boxtel, *Wageningen University*

Recommended Citation:

Djaeni, Mohamad; van Asselt, C. J.; Bartels, P. V.; Sanders, J. P. M.; van Straten, Gerrit; and van Boxtel, Anton J. (2011) "Low Temperature Drying With Air Dehumidified by Zeolite for Food Products: Energy Efficiency Aspect Analysis," *International Journal of Food Engineering*: Vol. 7: Iss. 6, Article 4.

DOI: 10.2202/1556-3758.1930

Available at: <http://www.bepress.com/ijfe/vol7/iss6/art4>

©2011 De Gruyter. All rights reserved.

Low Temperature Drying With Air Dehumidified by Zeolite for Food Products: Energy Efficiency Aspect Analysis

Mohamad Djaeni, C. J. van Asselt, P. V. Bartels, J. P. M. Sanders, Gerrit van Straten, and Anton J. van Boxtel

Abstract

Developments in low temperature drying of food products are still an interesting issue; especially with respect to the energy efficiency. This research studies the energy efficiency that can be achieved by a dryer using air which is dehumidified by zeolite. Experimental results are fitted to a dynamic model to find important variables for the drying operation. The results show that ambient air temperature as well as the ratio between air flow for drying and air flow for regeneration, affect the energy efficiency significantly. Relative humidity of used air, and shift time have a minor effect on the dryer performance. From the total work, it can be noted that the dryer efficiency operated at 50-60°C achieves 75 percent, which is attractive for drying of food products.

KEYWORDS: drying, adsorption, regeneration, energy efficiency, zeolite

Author Notes: This article is result of a collaboration between Diponegoro University and Wageningen University. The data of research was collected by experimental work at the System and Control Group, Agrotechnology and Food Science Wageningen University.

1. Introduction

Food products are sensitive to the heat load during drying. For example the color of tarragon (*Artemisia dracunculus L.*), as observed by Arabhosseini et al, 2009, changes to brown when drying occurs at too high temperatures. Furthermore, Mishkin et al, 1984, show that the degradation rate for vitamin C increases with temperature and at a product temperature of 50°C and a product moisture content of 2 kg water/kg dry matter, vitamin C content of the product degrades within a few minutes. Currently, more and more preprocessed vegetables are sold in Europe and the US. These products (lettuce, onions, carrots, cabbage, etc) are cut, washed and the excess of water is removed by drying before packing. Drying of these vegetables can only be done at low temperatures (15°C). If the product temperature becomes too high the color will change and the appearance quality goes down. Another example concern dried probiotics, where bacteria with a good effect on the digestion in the intestine are captured in a liquid matrix and spray dried. If the particle temperature is too high the bacterial activity degrades, and the product effectivity is lost. These are just some examples for a trend to low temperature drying of food products (see Ratti, 2001 and Djaeni, et al, 2009). Low temperature drying with air temperatures in the range 40-60°C, freeze drying and drying with air dehumidified by condensation are the common techniques for these products. The main limitations for these techniques are the high operational costs for freeze drying, and the low energy efficiency for the other methods (ranging between 10-40%).

An alternative to improve the drying capacity of air is by removing the vapor in the air used for drying by condensation or by using adsorbents (see Ratti, 2001; Zhang et al, 2007; Djaeni et al, 2009). Courtois, 2003 pointed that removal of vapor dehumidifies the air and thus improves the driving force for drying. Previous work referring to Ratti (2001) and Djaeni et al (2007a and 2009) showed that an adsorption dryer (where air is dehumidified by using adsorbents) has a higher potential for the reduction of energy usage and operational costs than a condensation dryer or freeze-dryer. Ratti, 2001 pointed that the total costs (fixed and operational cost for energy supply) of an adsorption dryer are about 50% below the total costs for a freeze-dryer. Djaeni et al (2009), conclude that the energy efficiency of an adsorption dryer operated below 50°C is 15-20% higher than that of a condensation dryer. Furthermore, Djaeni et al (2007b) also calculated that for drying at operation temperatures in the range of 60-80°C, the energy usage of adsorption dryer using zeolite can be half of the energy usage of a standard dryer working at comparable conditions.

Experimental work has been conducted to study the potential and effectiveness of several solid adsorbents for dehumidifying air to improve the driving force in drying processes. Witinantakit et al (2006) tested the performance

of paddy (rice) husk as vapor adsorbent in paddy drying and concluded that the drying rate was increased and a lower final paddy moisture content could be achieved by using dehumidified air. Nagaya et al (2006) improved the drying rate for vegetables (cabbage, egg plants and carrots) using air dehumidified by silica and could retain product quality attributes as color and vitamin. Revilla et al (2006) studied immersion drying of wheat using several adsorbents (alumina pillared clay, sand and zeolite) to speed up water evaporation, and Alikhan et al (1992) evaluated the potential of zeolite as adsorbent for drying corn in a rotary dryer. They found that zeolites have potential to increase the drying rate. Moreover, the capability of zeolites (4Å, 5Å and 13X) to dehumidify air has been tested and the results indicated that the vapor content in air can be reduced till a dew point of -60°C (see Kim et al, 2007). With this performance zeolite yields a far better dehumidification compared to common adsorbents as silica and alumina, and therefore zeolite is very important for adsorption drying.

Despite of the improvement of the drying rate and the release of adsorption heat, spent zeolite needs heat for its regeneration before reuse for air dehumidification. Improvements in the energy efficiency for the drying unit are (partly) cancelled by the energy requirement for regeneration.

In a preceding design studied by Djaeni et al (2007a and 2007b), an integrated system involving adsorber-regenerator, heater, dryer and heat recovery using a compressor and a heat exchanger network has been developed and evaluated with respect to the energy efficiency. The systems can be operated as a single-stage or a multi-stage system. The estimated efficiencies were compared with a conventional condensation dryer. For product drying at 20°C air inlet temperature the conventional dryer operated at an energy efficiency of 10% while the zeolite adsorbent dryer reached an efficiency of 23%, at 40°C air inlet temperature the values are respectively 28% and 50%, at 70°C air inlet temperature the values are respectively 63% and 90%.

This work is an experimental assessment of the energy efficiency for a single-stage dryer using zeolite for air dehumidification. The experimental data is fitted to a dynamic model for the experimental installation, and subsequently the model is used to predict the energy efficiency for a range of operational conditions. The study will contribute in how far the adsorption drying with zeolite can be beneficial for drying heat sensitive food product such as chili, soybean, tomato, vegetables, fruits, grains and coffee.

As this experimental work concerns the validation of the approach of adsorption drying with zeolites an electric heater (HE01) is used to heat up air for regeneration. B01 is a non-insulated column (inner diameter 0.15 m and 0.4 m height) to equalize temperature variations that occur after switching between adsorber and regenerator function. The buffer could be filled with alumina grid to make the buffering effect larger, but for the reported experiments the buffer was empty. HE02 is an additional electric heater to heat the dehumidified air from B01 up to the requested inlet dryer temperature. D01 is a tray dryer (cross sectional area 0.3x0.3m and height 0.4 m), where wet products are dried by dehumidified air. For these experiments sponges are used to imitate products which are in a constant drying rate period.

Sensors T-RH 1-3 (type HMP 130Y-O0205-4.3, VAISALA, Finland) are used to measure temperature and relative humidity of the air flows. F1 and F2 are air velocity sensors (SS 20.01/.011/0.12, SCHMIDT Feintechnik, Germany) to measure the linear velocity of air used for adsorption and regeneration. TH1-5 are K-type thermocouples (MB-ISK-S05-150-MP, Labfacility Ltd, United Kingdom) for temperature measurement.

2.2. Air dehumidification in a twin-column shift system

A fan is used to pass air at ambient conditions through the pipes (see Figure 1). The air is divided into two streams. The first stream is fed to the adsorber and adjusted by VF1, the other flow adjusted by VF2 enters HE01 and is heated up to above 110°C for the regenerator. In the adsorber (suppose column A), vapor is adsorbed from the air during contacting the zeolite bed, and thereby releasing heat which results a raised temperature leaving column A ($TH3 > TH2$). Air is then passed through HE02 to reach the drying temperature. Leaving HE02, the dehumidified air enters dryer (D01) to evaporate free water from the wet product.

Meanwhile, the hot air entering column B regenerates the spent zeolite. The hot air flow evaporates water from the saturated zeolite and as a result the outlet temperature of the regenerator is below the inlet temperature ($TH5 < TH4$). The exhaust air from the regenerator is not further used in this system, but from the measured temperature the heat recovery potential is calculated.

After completing a shift with continuous air flow the zeolite in column A will become nearly saturated with water. As a result, the adsorption effectiveness decreases. To continue air dehumidification the air for drying is switched to the column B with dry zeolite, while the saturated zeolite in column A is regenerated. As a consequence, the inlet and outlet point of adsorber-regenerator are also moved from TH2-TH3 to TH4-TH5.

2.3. Experimental conditions and data collection

In the experimental system the shift time, temperature of air for dryer and regenerator are manually controlled. The air flow is adjusted by regulating the valve positions VF1 for drying air, and VF2 for regenerator air. A program developed in LABVIEW and running on a PC is used to realize the setting values, to monitor drying, to collect experimental data and as a user interface. The data is recorded every two seconds. The data concerns:

- linear velocity of dryer air and regenerator air (F1 and F2),
- temperature of air entering adsorber and regenerator (TH2 or TH4) depending on shift),
- temperature of air exiting adsorber and regenerator (TH3 or TH5 depending on shift),
- relative humidity and temperature of ambient air (T-RH1),
- air exiting and entering dryer (T-RH2 and T-RH3).

By combining experimental data, the dimension of the pipes and physical properties of the components (air, zeolite, vapor, and water) the mass and energy flow of all the streams were calculated at each sampling moment. The data is used to calculate the energy efficiency of the system as presented in section 2.4.

Data was collected from the start-up of the installation. The first shift after start-up is regarded as a start shift for heating the installation and to regenerate the zeolite. Data from this shift is rejected for data processing. From the second shift the data is used for energy efficiency calculations, model fitting and validation.

Experiments concerned shift times 30, 45 and 60 minutes. Ambient air was used for the experiments. Temperature and humidity depended on the weather conditions and varied between 17-22°C, and 0.006-0.009 kg water/kg air. The inlet regeneration temperature was set to 140°C

2.4. Energy efficiency calculation

The heat efficiency of system is calculated based on Djaeni, et al (2007b):

$$\eta = \frac{Q_{evap}}{Q_{used} - Q_{rec,max}} 100\% \quad (1)$$

with Q_{evap} the total heat required for evaporating water from the material in the dryer (kJ) which follows from the inlet and outlet air humidity ($q_{v,d}^{in}, q_{v,d}^{out}$), and

the mass flow of dry air through the dryer ($F_{a,d}$) . For a total operational time tf , Q_{evap} corresponds to:

$$Q_{evap} = \int_{t=0}^{t=tf} F_{a,d} \Delta H_{evap} (q_{v,d}^{out} - q_{v,d}^{in}) dt \quad (2)$$

where, the values of humidity ($q_{v,d}^{in}, q_{v,d}^{out}$) are derived from the recorded temperature and relative humidity of air over an experiment (T-RH2 and T-RH3). The mass flow of dry air ($F_{a,d}$) is calculated from the recorded air flow according:

$$F_{a,d} = \frac{G_{a,d}}{1 + q_{v,d}^{in}} \quad (3)$$

with $G_{a,d}$ the mass flow of wet air (kg/minute) derived from the air velocity measurement (F1) multiplied with the cross sectional area of the pipe and air density.

Q_{used} is the total of heat introduced to system (kJ) and equals the heat supplied to the regenerator and the heat to bring the dehumidified air from the adsorber to the drying temperature:

$$Q_{used} = \int_{t=0}^{t=tf} (F_{a,reg} cp_{a,reg} (T_{a,reg}^{in} - T_{amb}) + F_{a,ad} cp_{a,ad} (T_{a,d}^{in} - T_{a,ad}^{out})) dt \quad (4)$$

with $F_{a,ad}$ as the dry air flow entering the adsorber and equals to $F_{a,d}$. $F_{a,reg}$ is calculated analog to equation 3 using the data from measurement device F2, $T_{a,reg}^{in}$ follows from TH2 or TH4 depending on the shift, T_{amb} and $T_{a,d}^{in}$ are measured by T-RH1 and T-RH2, respectively. Finally, $T_{a,ad}^{out}$ is measured by TH3 or TH5 and depends on the shift.

$Q_{rec,max}$ is the calculated amount of heat which could be recovered from the exhaust air of the regenerator (kJ). The recovery is based on a heat exchanger with 10°C temperature difference between hot and cold stream. The maximum recovered heat is set to:

$$Q_{rec,max} = \int_{t=0}^{t=tf} F_{a,reg} c_{p,a,reg} (T_{a,reg}^{out} - T_{amb} - 10) dt \quad (5)$$

Here, $T_{a,reg}^{out}$ is measured from TH3 or TH5 and depends on the shift.

3. Model Development

3.1. Assumptions

The model in the form of partial differential equations is set up to predict the energy efficiency of the zeolite dryer for process conditions which are beyond the experimental range of the installation. The model is based on mass and energy balances for air and solids in the adsorber, regenerator and dryer. Figure 2 gives a schematic presentation of the flows. Temperatures for air, zeolite and product, as well as moisture in air, zeolite and product are a function of the vertical dimension (h). For the balances moisture and energy exchange between air and solid material is considered and also heat loss due to temperature differences between the air in the equipment and air in the environment. Moreover, heat released during adsorption and heat required for regeneration is taken into account.

The model is based on the following assumptions:

1. the flow of air through the bed of adsorbent is plug flow,
2. pressure drop over the equipment is neglected,
3. physical constants as density, specific heat, and diffusion coefficients are constant,
4. only the dynamics and spatial distribution in the adsorber, dryer and regenerator are considered; responses for heater, and pipes are instantaneous,
5. the free water of imitated product in dryer is in excess and so that the dryer operates in a constant drying rate period,
6. adsorption heat is equal to desorption heat,
7. the model includes heat loss from adsorber, regenerator and dryer to the environment,
8. water and heat transport between zeolite and product particles take place through the air and not by particle contact.

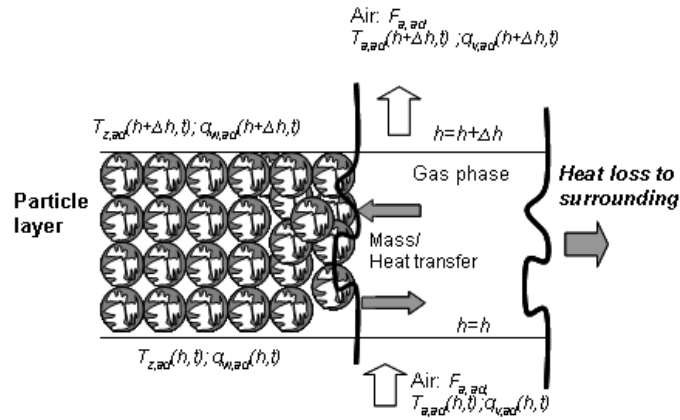


Figure 2: Spatial representation for adsorber, regenerator and dryer

3.2. Model formulation

Table 1 presents the dynamic mathematical model describing the phenomena in each equipment unit with symbol notation depicted in table A.1, appendix. The model is completed by the additional equations as depicted in table 2. Initial values and boundary conditions are given in table A.2 (appendix).

Table 1: Dynamic model of the adsorption dryer system**Adsorber**

Mass balance of water

$$\text{Zeolite: } \frac{dq_{w,ad}(h,t)}{dt} = r_{ads}(h,t) \quad (6)$$

$$\text{Air: } \varepsilon_z \frac{dq_{v,ad}(h,t)}{dt} = -\left(\frac{F_{a,ad}}{\rho_a A_{col}}\right) \frac{dq_{v,ad}(h,t)}{dh} - \frac{\rho_z}{\rho_a} (1 - \varepsilon_z) r_{ads}(h,t) \quad (7)$$

Heat balance

$$\text{Zeolite: } \rho_z c_{p,z,ad} (1 - \varepsilon_z) \frac{dT_{z,ad}(h,t)}{dt} = \rho_z (1 - \varepsilon_z) \Delta H_{ads} r_{ads}(h,t) - U_z S_{A,z} (T_{z,ad}(h,t) - T_{a,ad}(h,t)) \quad (8)$$

Air:

$$\rho_a c_{p,a,ad} \varepsilon_z \frac{dT_{a,ad}(h,t)}{dt} = -\frac{F_{a,ad} c_{p,a,ad}}{A_{col}} \frac{dT_{a,ad}(h,t)}{dh} + U_z S_{A,z} (T_{z,ad}(h,t) - T_{a,ad}(h,t)) - \frac{4U_{bed,col}}{ID_{col}} (T_{a,ad}(h,t) - T_{amb}) \quad (9)$$

Regenerator

Mass balance of water

$$\text{Zeolite: } \frac{dq_{w,reg}(h,t)}{dt} = r_{des}(h,t) \quad (10)$$

$$\text{Air: } \varepsilon_z \frac{dq_{v,reg}(h,t)}{dt} = -\left(\frac{F_{a,reg}}{\rho_a A_{col}}\right) \frac{dq_{v,reg}(h,t)}{dh} - \frac{\rho_z}{\rho_a} (1 - \varepsilon_z) r_{des}(h,t) \quad (11)$$

Heat balance

$$\text{Zeolite: } \rho_z c_{p,z,reg} (1 - \varepsilon_z) \frac{dT_{z,reg}(h,t)}{dt} = \rho_z (1 - \varepsilon_z) \Delta H_{des} r_{des}(h,t) - U_z S_{A,z} (T_{z,reg}(h,t) - T_{a,reg}(h,t)) \quad (12)$$

Air:

$$\rho_a c_{p,a,reg} \varepsilon_z \frac{dT_{a,reg}(h,t)}{dt} = -\frac{F_{a,reg} c_{p,a,reg}}{A_{col}} \frac{dT_{a,reg}(h,t)}{dh} + U_z S_{A,z} (T_{z,reg}(h,t) - T_{a,reg}(h,t)) - \frac{4U_{bed,col}}{ID_{col}} (T_{a,reg}(h,t) - T_{amb}) \quad (13)$$

Dryer

Mass balance of water

$$\text{product: } \frac{dq_{w,d}(h,t)}{dt} = -r_{dry}(h,t) \quad (14)$$

$$\text{Air: } \varepsilon_p \frac{dq_{v,d}(h,t)}{dt} = -\left(\frac{F_{a,d}}{\rho_a A_d}\right) \frac{dq_{v,d}(h,t)}{dh} - \frac{\rho_p}{\rho_a} (1 - \varepsilon_p) r_{dry}(h,t) \quad (15)$$

Heat balance

$$\text{Product: } \rho_p c_{p,p,d} (1 - \varepsilon_p) \frac{dT_{p,d}(h,t)}{dt} = \rho_p (1 - \varepsilon_p) \Delta H_v r_{dry}(h,t) - U_p S_{A,p} (T_{p,d}(h,t) - T_{a,d}(h,t)) \quad (16)$$

$$\text{Air: } \rho_a c_{p,a,d} \varepsilon_p \frac{dT_{a,d}(h,t)}{dt} = -\frac{F_{a,d} c_{p,a,d}}{A_d} \frac{dT_{a,d}(h,t)}{dh} + U_p S_{A,p} (T_{p,d}(h,t) - T_{a,d}(h,t)) - \frac{U_{bed,d}}{l_d} (T_{a,d}(h,t) - T_{amb}) \quad (17)$$

Table 2: Additional equations related to equations 6 to 17

Adsorber	$r_{ads}(h,t) = k_{ads}(q_{e,ad}(h,t) - q_{v,ad}(h,t))$ $k_{ads} = C_1(T_{z,ad}(h,t) + 273.15)$ $q_{e,ad}(h,t) = C_2 \left[\tanh(\log_{10}(P_{v,ad}(h,t)) + C_3 T_{z,ad}(h,t)) + 1 \right]; C_2 = 0.1132; C_3 = -0.0266$ <p>The equilibrium moisture loaded in zeolite is a function of vapor partial pressure and temperature derived from zeolites properties in CECA data sheet^[14].</p> $P_{v,ad}(h,t) = \frac{y_{v,ad}(h,t)}{1 + y_{v,ad}(h,t)} P_{total}; y_{v,ad}^i = \frac{q_{v,ad}(h,t) / 0.622}{1 + q_{v,ad}(h,t) / 0.622}$ $A_{col} = \frac{\pi}{4} (ID_{col})^2; S_{A,z} = S_{pa,z} \rho_z; F_{a,ad} = \frac{G_{a,ad}}{1 + q_{v,amb}}; G_{a,ad} = F_1 A_{col} \rho_a$ <p>F_1 is linear velocity of air entering adsorber measured from F1</p> $cp_{z,ad} = cp_z + cp_w q_{w,ad}(h,t); cp_{a,ad} = cp_a + cp_v q_{v,ad}(h,t)$
Regenerator	$r_{des} = -k_{des}(q_{e,reg}(h,t) - q_{v,reg}(h,t))$ $k_{des} = C_4(T_{z,reg}(h,t) + 273.15)$ $\Delta H_{des} = \Delta H_{ads}$ $cp_{z,reg} = cp_z + cp_w q_{w,reg}(h,t); cp_{a,reg} = cp_a + cp_v q_{v,reg}(h,t);$ $F_{a,reg} = \frac{G_{a,reg}}{1 + q_{v,amb}}; G_{a,reg} = F_2 A_{col} \rho_a$ <p>F_2 is linear velocity of air entering regenerator measured from F2</p>
Dryer	$r_{dry} = -k_{d0}$ $cp_{p,d} = cp_p + cp_w q_{w,d}(h,t); cp_{a,d} = cp_a + cp_v q_{v,p}(h,t)$ $F_{a,d} = F_{a,ad}$ $A_d = w_d l_d; V_d = w_d l_d h_d; S_{A,p} = S_{pa,p} \rho_p w_d l_d h_d$

4. System Behaviour

4.1. Parameter estimation

Equations 6 to 17 with the additional equations depicted in table 2 were solved using the boundary and the initial conditions as given in table A.2 (appendix), and using the equipment dimensions, material properties, and the process constants as given in table A.3 (appendix).

The measured values of the flows and inlet temperatures during the operational time were used as input data for the model. The model responses in time were fitted to the experimental measured values of temperature and humidity of the air leaving the adsorber, temperature of air leaving the regenerator, and

temperature and humidity of air leaving the dryer. For response fitting and parameter estimation Matlabs' function *fmincon* is used.

The model equations 1-17 contain several physical and kinetic constants which are known from handbooks or product data sheets. The unknown parameters in the set of equations are C_1 , C_4 (adsorption and desorption rate constants), $U_{bed,col}$, $U_{bed,d}$ (overall heat transfer coefficients for heat exchange between the columns/dryer and the environment), and k_{d0} (drying rate constant). The estimation of these parameters could partly be separated; i.e. parameters for the adsorber, for the regenerator and for the dryer. The procedure followed the next steps:

1. C_1 was obtained by minimization the sum of squared error (SSE) of humidity of air leaving the adsorber

2.

$$SSE_{ad} = \sum_{t=t0}^{t=tf} (q_{v,ad}^{experiment} - q_{v,ad}^{model})^2 \quad (18)$$

$q_{v,ad}^{experiment}$ was obtained from the relative humidity and temperature of sensor

T-RH2 and $q_{v,ad}^{model}$ from equation 7

3. $U_{bed,col}$ was obtained by minimization of the sum of squared error (SSE) of temperature of air leaving the adsorber

$$SSE_{ad} = \sum_{t=t0}^{t=tf} (T_{a,ad}^{experiment} - T_{a,ad}^{model})^2 \quad (19)$$

$T_{a,ad}^{experiment}$ was obtained from the temperature sensors TH3 or TH5 depending

on the shift and $T_{a,ad}^{model}$ from equation 9

4. C_4 was obtained by minimization of the sum of squared error (SSE) of the temperature of air leaving the regenerator (analog to equation 19)
5. k_{d0} followed from minimization of the sum of squared error (SSE) of humidity of air leaving the dryer (analog to equation 18)
6. $U_{bed,d}$ followed from the minimization of sum of squared error (SSE) of temperature of air leaving the dryer (analog to equation 19)

Estimated parameter values are given in table 3. The values for the overall heat transfer coefficient of zeolite, and the values of the adsorption and desorption rate are comparable to that of Gorbach et al, 2004 Jenkins et al, 2002, and Anonymous, 2006. The values also match with the zeolite specification. However, the values of drying rate and evaporation capacity by zeolite are above the values given in the literature and which range from 0.0005 to 0.0025 depending on type

of dryer and product (see Arabhosseini, et al 2005; Mustafa et al, 2009, Holmberg and Ahtila, 2004, Baker et al, 2006 and Temple, 2000).

Table 3: Estimated parameters

Parameter	Dimension	Estimated values
$C_1; C_4$	1/minute K	$0.12 \times 10^{-3}; 0.6 \times 10^{-3}$
$U_{bed,col}; U_{bed,d}$	$\text{kJ/m}^2 \text{ min}^\circ\text{C}$	1.250; 0.002
k_{d0}	1/minute	0.14×10^{-2}

4.2. Profiles for water content and temperature in air, zeolite and product

Figure 3 to 5 present the measurements and model results for a shift time of 60 minutes over 4 shift periods. Initially, a mismatch between the measured air humidity and the modeled air humidity was observed. However, it was recognized that the response time of the relative humidity sensors was not a part of the model. Separate measurements on the relative humidity sensors showed that the sensors had a 63% response time of 2 minutes. This behavior was added to the model by a first order differential equation with a time constant of 2 minutes:

$$2 \frac{dRh_{meas}}{dt} + Rh_{meas} = Rh.$$

Figure 3 gives the measurements for the air at inlet (*) and outlet (o) of the adsorber. For every shift, during a few minutes the moist air which is left after regeneration is moved from the adsorber (phase 1). Then the adsorber reduces the water content in the air over 90% for a period of 40 minutes (see phase 2 in Figure 3a). After this period, the water uptake capacity of the zeolite in adsorber decreases as the zeolite approaches saturation, and as a result, the humidity of air at outlet of the adsorber increases (phase 3).

After regeneration the piping material towards the column is hot. As a consequence the inlet temperature starts at 45°C and decreases gradually in time. Due to the heat buffering capacity of the zeolite, the temperature at the outlet of the adsorber starts around 110-120°C (see Figure 3b), i.e. the temperature of the zeolite after regeneration. In the first minutes of an adsorption shift, the zeolite is cooled (phase 1). Subsequently, the temperature remains on a level of 60-70°C due to the release of adsorption heat (phase 2). Towards the end of a shift the temperature falls because the zeolite becomes saturated and thus the release of adsorption heat goes down (phase 3). Finally, the air temperature at the outlet of the adsorber is close to the adsorber inlet temperature (*).

The measured data was fitted to the model by estimating the adsorption rate constant (C_1) and the overall heat transfer coefficient between column and environment ($U_{bed,ad}$), see also table 3. Figures 3a and 3b show that the humidity

and temperature of air leaving the adsorber obtained by the model (—) and experiment (o) are close. The measured humidity deviates direct after the switches slightly from the model due to the response time of the humidity sensor which reacts with a first order response of 2 minutes. If this response would be included in the model a nearly perfect match could be obtained in this phase of the responses.

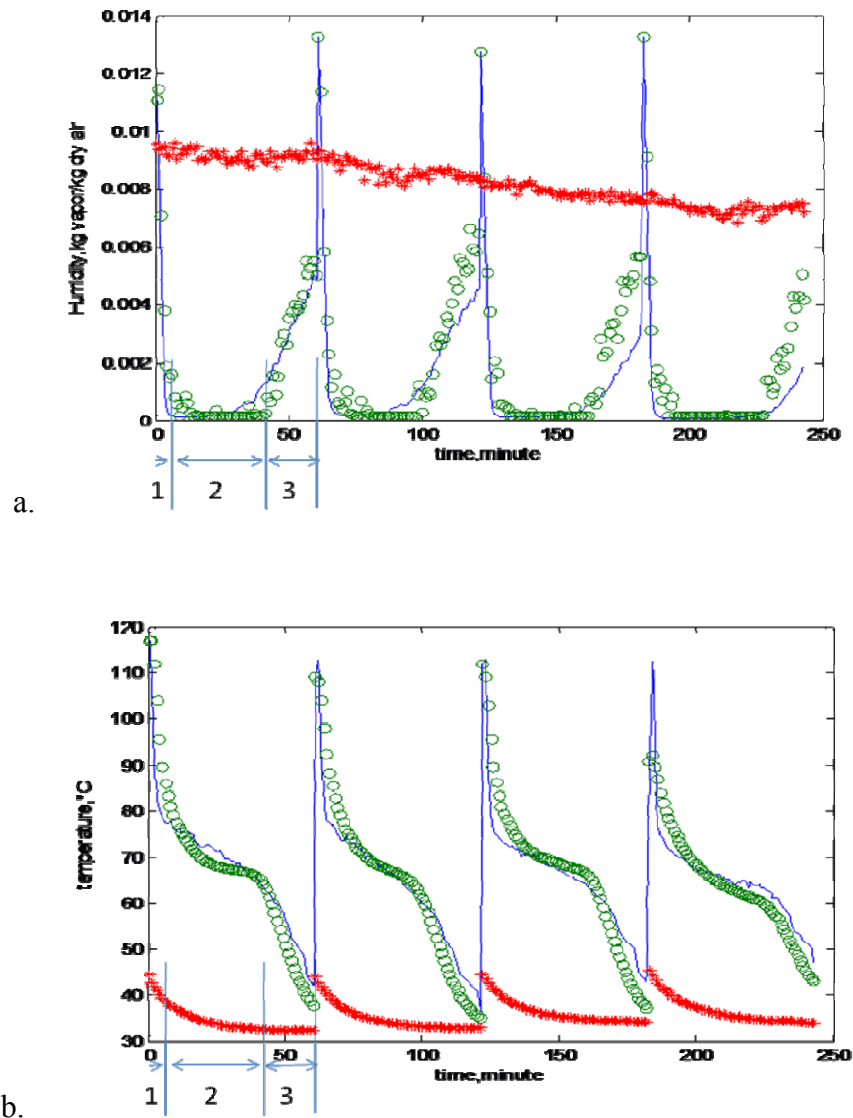


Figure 3: Conditions of air at the entrance (*) and exhaust of the adsorber (o experiment, — model). a: recorded humidity, b: recorded temperature

The inlet and exhaust air temperature for the regeneration shift are presented in Figure 4. First, it is noted that the inlet temperature of the regenerator (*) starts at 110°C and increases gradually to 140°C; i.e. the temperature after the heater. This typical response is result of heating-up pipe walls and metal valves between the electrical heater and the entrance of the regenerator. The heat capacity of these components is considerable compared to the heat content of the air flow.

Next, the experimental results show that in the initial 1-2 minutes after switching the regenerator exhaust temperature increases slightly from the temperature which was achieved at the end of the adsorption shift. This effect is result of an initial heating-up of the zeolite. Between 2-10 minutes, the energy is used to release water from the zeolite. Thus, in this period the temperature at the outlet of the regenerator hardly changes. After this period of about 10 minutes less water is removed from the zeolite and as a result the temperature difference between in and outlet of the regenerator becomes smaller. At the end of the shift there is still a temperature difference between inlet and outlet as a result of the heat loss which occurs despite the insulation of the columns.

The air temperature at the outlet was fitted to the model by adjustment of the regeneration rate constant (C_4). Model and experimental results are nearly the same.

Remark: water removal could be improved by a higher regeneration temperature, but the equipment was limited in its experimental range.

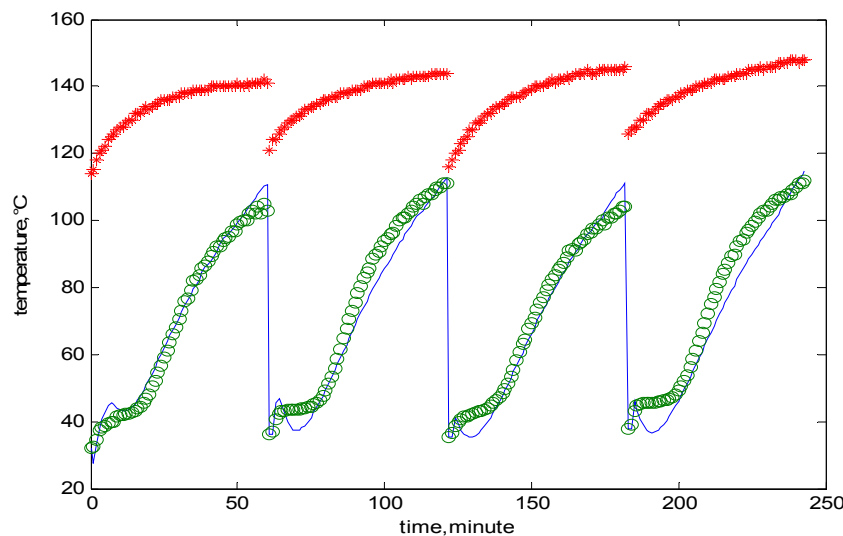


Figure 4: Temperature of air: (*) entering and exiting the regenerator (— model, o experiment)

Figure 5 shows the humidity of air at inlet and outlet of the regenerator. The inlet humidity is based on measurements of the ambient humidity, whereas the outlet humidity is reconstructed from the model by using the estimated parameters given in table 3. The humidity of air leaving the regenerator is for about 2 minutes close to the last value from the adsorber shift. After 2 minutes the humidity increases and the water removal from the zeolite is the highest and later on the water removal decreases during of time. At the end of the shifts the humidity of air exiting the regenerator is close to the inlet humidity (*) which indicates that regeneration is not longer effective.

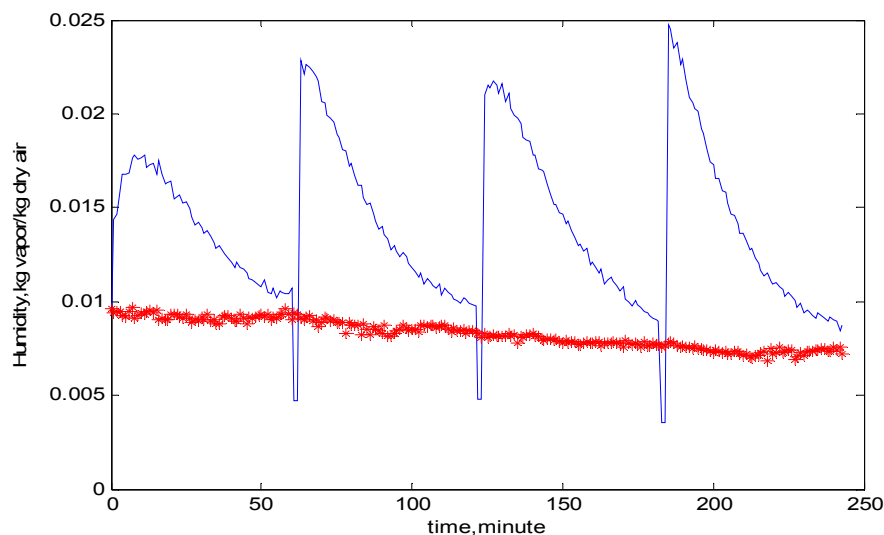


Figure 5: Measured humidity of air entering (*) the regenerator and model based reconstruction of humidity at the exhaust of the regenerator (-)

Results for the dryer are illustrated in Figure 6. The dehumidified air from the absorber is used as drying medium, but before entering the dryer the air passes the buffer B01, which was not insulated, and the heater HE02 operated at a low constant heating input. Despite the absence of buffering material, the buffer equalizes the temperature and as a result the inlet temperature for the dryer is nearly constant and varies between 52.0-55.0°C.

During these experiments wet product was dried. The vapor pressure of water in the product was high compared to that of the air. As a result, product is dried with a constant drying rate over the whole shift period. The humidity of air at the outlet of the dryer is related to the response of the humidity of air after the adsorber (see Figure 6a). From the inlet and outlet humidity follows that the drying capacity of air is indeed constant. With the estimated drying rate constant

and overall heat transfer coefficient between dryer wall and environment (see table 3) good correspondence between model and experiment is obtained.

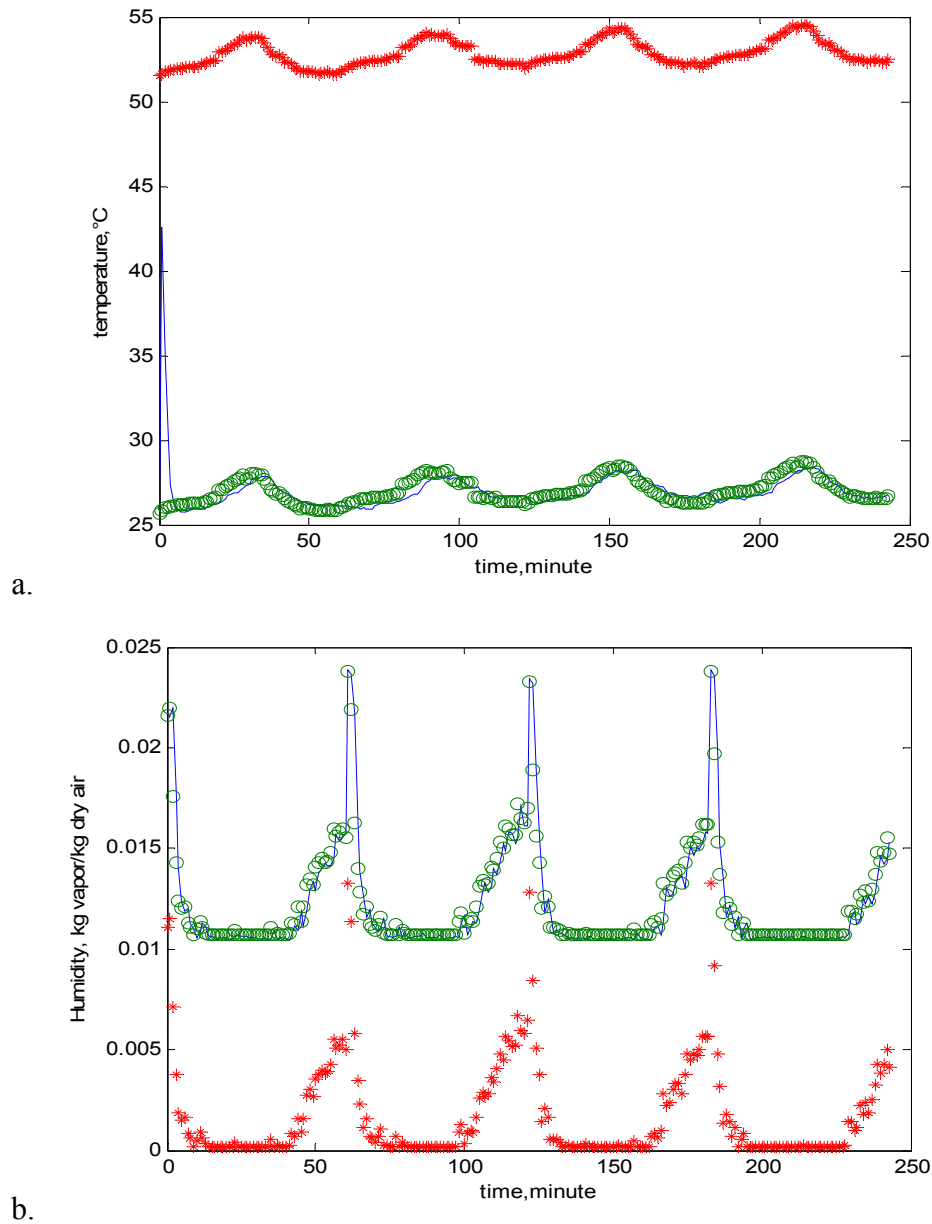


Figure 6: Conditions for air entering (*) and exiting the dryer (° experiment and ___ model, a: air temperature, b: air humidity)

4.3. Efficiency calculation

Experimental data of a series of shifts were used to calculate the energy efficiencies according equation 1 to 5. The energy efficiency was also calculated from the fitted dynamic model (equation 6-17). Moreover, a comparison was made with model results for a continuous dryer with air dehumidification with zeolite. As that system was in a continuous operation mode a steady state model concerning overall mass and energy balances of the adsorber, regenerator and dryer was used referring to Djaeni et al, 2007a. The operational conditions recorded during the experiments were used as input for the efficiency calculations with the steady-state model.

The results in table 4 show that the experimentally obtained heat efficiency is close to that of the model predictions (Djaeni et al, 2007a and Djaeni et al 2008). It is also observed that for a longer shift time the experimentally obtained results come closer to the results of the models.

Table 4: Efficiency of the adsorption dryer system at flow of air dryer 1.70 kg/minute and air regenerator 1.90 kg/minute

Shift Time, min	Efficiency, (%)		
	Experimental	Dynamic Model*	Steady state model**
30	50.4	49.7	53.20
45	52.7	51.6	53.90
60	53.9	52.8	54.80

*see Djaeni et al, 2008

**Djaeni, et al, 2007a

5. Sensitivity Analysis

The experiments were done for a range of conditions that could be realized with the experimental installation. As the model is based on laws of conservation it allows extrapolating the other operational conditions and so the model is used to investigate the effect of drying conditions on the energy efficiency.

5.1. Effect air flow ratio and shift time

The experimental installation functions the best for a 1:1 ratio between the air flow for adsorption/drying and air flow for regeneration. With higher flow rates fluidization and entrainment of the particles occurred. Figure 7 shows that the energy efficiency increases if the ratio between the air flow for drying and air flow for regeneration increases. At a ratio 3.5-4.0:1 the efficiency is 70-72% which is similar to the calculations results in the previous study using a steady-state model and a flow ratio 4:1(Djaeni et al, 2007a). This ratio is result of the fact

that hot air used for water removal from zeolite at 110-140°C can contain over 4 times more water than moderately heated air for water removal from the product at 50°C.

The shift time also affects the energy efficiency and the best performance is obtained for a shift time of 60 minutes. Main reason is that for a short shift time (for example 30 minutes) the zeolite is not sufficiently regenerated, which lowers the efficiency of the zeolite for air dehumidification over a series of shifts.

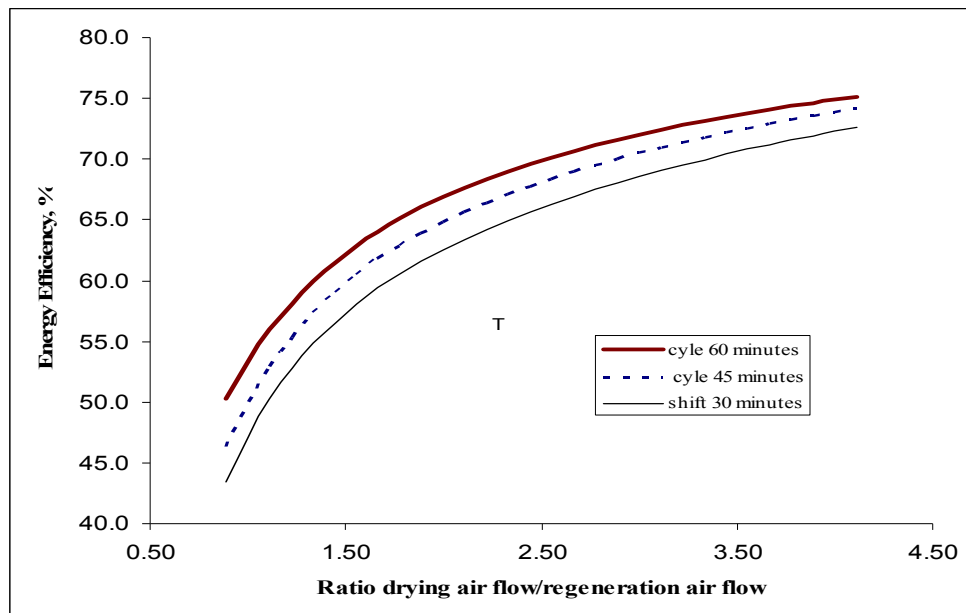


Figure 7: Effect of ratio drying air flow/regeneration air flow. Shift times 30, 45, 60 minutes, ambient temperature 20°C, RH 40%

5.2. Properties of ambient air used for drying

For a higher moisture content in the inlet air, the time until the zeolite becomes saturated is shorter, but the total amount of released heat remains the same. As a consequence, the relative humidity of ambient air used for drying has not much effect on the energy efficiency (see figure 8).

The temperature of the ambient air used for drying affects the energy efficiency significantly (see figure 9); a higher ambient air temperature is beneficial because:

- A higher ambient temperature yields an almost an equally higher temperature of air from the adsorber. Hence, the required energy to heat the dehumidified air to the dryer temperature decreases.

- In a similar way the energy to heat ambient air to the regeneration temperature is lower. Moreover, there is some advantage from the higher temperature of the spent zeolite at the end of the adsorption shift which requires less energy to achieve the regeneration temperature.
- Heat loss from air in the equipment to the environment is lower.

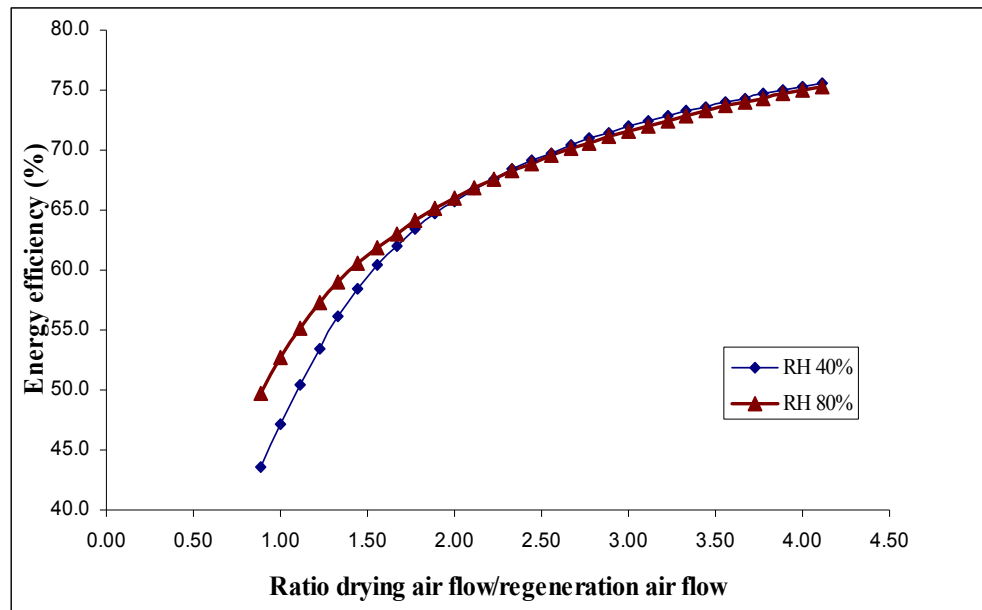


Figure 8: Effect of ratio drying air flow/regeneration air flow. Shift time 45 minutes, RH 40%, 80% and ambient temperature 20°C

Conclusion

In this work the energy efficiency of a single-stage system is experimentally evaluated in a twin-column system with zeolite as adsorbent. The twin-columns are alternately used for air dehumidification and for zeolite regeneration.

The experimental results yielded energy efficiencies in the range 50-55%. The energy efficiency for conventional dryers at the same operational conditions are around 30%. Application of the experimental conditions to the steady-state model used in the previous study resulted in energy efficiencies values which correspond to the obtained experimental results. So, the steady state model gives reliable predictions of the energy efficiency which can be realized.

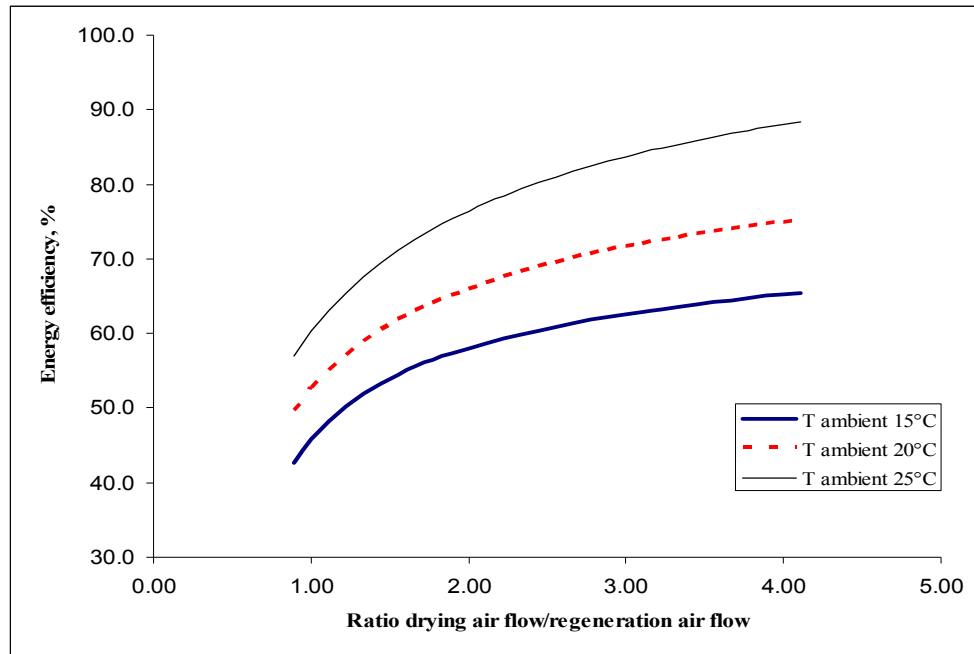


Figure 9: Effect of ratio drying air flow/regeneration air flow. Shift time 45 minutes, RH 40% and varying ambient temperature at 15, 20 and 25°C

To be able to extrapolate the experimental results to other operational conditions the experimental results were fitted to a dynamic model of the twin-column system. A sensitivity study for the main process variables on this model indicated that the ratio between air flow used for drying and air flow used for regeneration affects the energy efficiency significantly. If this ratio is 4:1, (as applied in previous study) an energy efficiency of 70-75% is obtained, which corresponds to the result of previous work. Other important variables that affect the efficiency are the temperature of air used for drying and the shift time.

The experimental work confirms that model predictions from previous work are accurate. The work confirms also the potential of the reduction of energy usage during low temperature drying of food products like herbs, vegetables and probiotics by using zeolite for air dehumidification. In the next research, the food products and the obtained quality will be evaluated in the dryer. The efficiency improvement follows from the heat recovery potential from the regenerator exhaust air. Therefore, similar results will be achieved for energy usage from other sources (biofuel, biogas or solar).

Appendix

Table A.1: List and notation of symbols

A	cross sectional area	(m ²)
$C_{1,2,...n}$	equilibrium and kinetic constant	
F	flow of dry component	(kg/min)
G	flow of wet component	(kg/min)
ID	internal diameter	(m)
P	total pressure	(bar)
Q	heat flow	(kJ/min)
R	gas constant	(kJ/kmole K)
RH	relative humidity	(%)
S_{pa}	specific surface area	(m ² /kg)
T	temperature	(°C)
U	overall heat transfer coefficient	(kJ/m ² min °C)
V	volume	(m ³)
cp	specific heat	(kJ/kg°C)
h	height in adsorbent	(m)
h_{ad}, h_d, h_{reg}	total height of adsorber, dryer, regenerator	(m)
k	constant of water transfer rate	(1/min)
l_d	length of dryer	(m)
q	water content in dry matter	(kg water/kg dry matter)
r	rate of water transfer	(kg water/kg dry matter/ min)
t	time	(min)
tf	final time	(min)
w_d	width of dryer	(m)
y	vapor in air	(kmole/kg dry air)
ΔH	latent heat of water change	(kJ/kg)
ρ	density	(kg/m ³)
η	energy efficiency	(%)
ε	porosity of material	

Subscripts					
a	air	ad	adsorber	ads	adsorption
amb	ambient	c	cycle	col	column
d	dryer	des	desorption	dry	drying
e	equilibrium	$evap$	evaporation	in	inlet
max	maximum	out	outlet	p	product
reg	regenerator	rec	recovered	req	required
$used$	used	v	vapour	w	water
z	zeolite				

Table A.2: Boundary condition and initial condition

Adsorber	parameter	Position (h)	Boundary condition	Initial condition See Table A.2, appendix
	$q_{v,ad} ; T_{a,ad}$	0	$q_{v,ad}(0,t) = q_{v,amb} ; T_{a,ad}(0,t) = T_{amb}$	$q_{v,ad}(h,0) = q_{v,reg}(h,t_c)$
	$q_{w,ad} ; T_{z,ad}$		$\frac{dq_{w,ad}(0,t)}{dt} ; \frac{dT_{z,ad}(0,t)}{dt}$ (analog eq.6 & 8)	$q_{w,ad}(h,0) = q_{w,reg}(h,t_c)$
	$q_{v,ad} ; T_{a,ad}$	h_{ad}	$\frac{dq_{v,ad}(h_{ad},t)}{dt} ; \frac{dT_{a,ad}(h_{ad},t)}{dt}$ (analog eq. 7&9)	$T_{a,ad}(h,0) = T_{a,reg}(h,t_c)$
	$q_{w,ad} ; T_{z,ad}$		$\frac{dq_{w,ad}(h_{ad},t)}{dt} ; \frac{dT_{z,ad}(h_{ad},t)}{dh}$ (analog eq. 6&8)	$T_{z,ad}(h,0) = T_{z,reg}(h,t_c)$
			$T_{a,ad}^{out} = T_{a,ad}(h_{ad},t) ; q_{v,ad}^{out} = q_{v,ad}(h_{ad},t)$	
Regenerator	$q_{v,reg} ;$	0	$q_{v,reg}(0,t) = q_{v,amb} ; T_{a,reg}(0,t) = T_{a,reg}^{in}$	$q_{v,reg}(h,0) = q_{v,ad}(h,t_c)$
	$T_{a,reg}$		$\frac{dq_{w,reg}(0,t)}{dt} ; \frac{dT_{z,reg}(0,t)}{dt}$ (analog eq. 10 & 12)	$q_{w,reg}(h,0) = q_{w,ad}(h,t_c)$
	$q_{w,reg} ;$			$T_{a,reg}(h,0) = T_{a,ad}(h,t_c)$
	$T_{z,reg}$			$T_{z,reg}(h,0) = T_{z,ad}(h,t_c)$
	$q_{v,reg} ;$	h_{reg}	$\frac{dq_{v,reg}(h_{reg},t)}{dt} ; \frac{dT_{a,reg}(h_{reg},t)}{dh}$ (analog eq. 11&13)	
	$T_{a,reg}$		$\frac{dq_{w,reg}(h_{reg},t)}{dt} ; \frac{dT_{z,reg}(h_{reg},t)}{dt}$ (analog eq. 12)	
	$q_{w,reg} ;$			
	$T_{z,reg}$		$T_{a,reg}^{out} = T_{a,reg}(h_{reg},t) ; q_{v,reg}^{out} = q_{v,reg}(h_{reg},t)$	
Dryer	$q_{v,d} ; T_{a,d}$	0	$q_{v,d}(0,t) = q_{v,ad}(h_{ad},t) ; T_{a,d}(0,t) = T_{a,d}^{in}$	$q_{v,d}(h,0) = q_{v,ad}(h_{ad},t_c)$
	$q_{w,d} ; T_{p,d}$		$\frac{dq_{w,d}(0,t)}{dt} ; \frac{dT_{p,d}(0,t)}{dt}$ (analog eq. 14 & 16)	$q_{w,d}(h,0) = q_{w,d}^0$
	$q_{v,d} ; T_{a,d}$	h_d	$\frac{dq_{v,d}(h_d,t)}{dh} ; \frac{dT_{a,d}(h_d,t)}{dt}$ (analog eq. 15& 17)	$T_{a,d}(h,0) = T_{a,d}^0$
	$q_{w,d} ; T_{p,d}$		$\frac{dq_{w,d}(h_d,t)}{dt} ; \frac{dT_{p,d}(h_d,t)}{dt}$ (analog eq. 14& 16)	$T_{p,d}(h,0) = T_{p,d}^0$
			$T_{a,d}^{out} = T_{a,d}(h_d,t) ; q_{v,d}^{out} = q_{v,d}(h_d,t)$	

Table A.3: Material properties and equipment data

Notation	Parameter	Value	
$h_{ad}; ID_{ad}$	Height and inside diameter of adsorber, m	0.24;0.15	
ID_{pipe}	inside diameter of pipe, m	0.05	
$w_d;l_d;h_d$	Width, length and height of dryer, m	0.3;0.3;0.4	
	Weight of zeolite used (gram)	2500	
$S_{pa,z};S_{pa,p}$	Specific surface area of zeolite and product (m ² /g), see Gorbach et al, 2004)	20; 20	
t	Time, minute		
Properties			
$\varepsilon_z;\varepsilon_p$	Porosity of zeolite and product in bed	0.3;0.4	
ρ_z	Density of zeolite (kg/m ³), see Gorbach et al, 2004	736.5	
ρ_p	Density of product (kg/m ³)	36	
ρ_a	Density of air (kg/m ³)	1.08	
$U_z;U_p$	Overall heat transfer of zeolite (see Jenkins et al, 2002); product, kJ/m ² min°C	0.116	
ΔH_{ads}	Latent heat of water adsorption (kJ/kg) see Gorbach et al, 2004	4400	
cp_v	Specific heat of vapor (kJ/kg °C)	1.93	
cp_a	Specific heat of dry air (kJ/kg °C)	1	
cp_w	Specific heat of water (kJ/kg °C)	4.2	
cp_p	Specific heat of dry product (kJ/kg °C), see Gorbach et al, 2004	0.920	
ΔH_v	Latent heat of water evaporation (kJ/kg)	2500	
Input condition			
$G_{air,ad}$	Flow rate of air for adsorber or dryer, kg/h	1.70	
$G_{air,reg}$	Flow rate of air for regenerator, kg/h	2.00	
T_{amb}	Ambient temperature (measured), °C	17-20	
RH_{amb}	Ambient relative humidity (measured), %	35	
$q_{v,amb}$	Humidity of ambient air	0.0065- 0.0080	
$T_{a,reg}$	Temperature of inlet regenerator	120	
$T_{a,d}^{in}$	Temperature of inlet dryer	50	
Initial condition for shift 1 (first shift)			
$q_{w,ad}(h,0)$	Adsorber	Water in zeolite, kg water/kg dry zeolite	0.025
$T_{z,ad}(h,0)$		Temperature of zeolite, °C	40
$q_{v,ad}(h,0)$		Humidity of air, kg vapor/kg dry air	0.008
$T_{a,ad}(h,0)$		Temperature of air, °C	40
$q_{w,ad}(h,0)$	Regenerator	Water in zeolite, kg water/kg dry zeolite	0.16
$T_{z,reg}(h,0)$		Temperature of zeolite, °C	80
$q_{v,reg}(h,0)$		Humidity of air, kg vapor/kg dry air	0.008
$T_{a,reg}(h,0)$		Temperature of air, °C	120
$q_{w,d}(h,0)$	Dryer	Water content in product, kg water/kg dry product	10
$T_{p,d}(h,0)$		Temperature of product, °C	18
$q_{v,d}(h,0)$		Humidity of air, kg vapor/kg dry air	0.001
$T_{a,d}(h,0)$		Temperature of air, °C	50

References:

- Alikhan, Z.; Raghavan, G.S.V.; Mujumdar, A.S. Adsorption drying of corn in zeolite granules using a rotary drum. *Drying Technology* **1992**, 10(3); 783-797
- Anonymous. Zeolite:Datasheet.
<http://www.cecachemicals.com/sites/ceca/en/home.page> (accessed September 26, 2006)
- Arabhosseini, A.; Huisman, W. ; van Boxtel, A.; Muller, J. Modeling of the Equilibrium Moisture (EMC) Tarragon (*Artemisia Dracunculus L.*). *International Journal of Food Engineering* **2005**, 1(5), article 7
- Arabhosseini, A., Padhye, S., Huisman, W., van Boxtel A.J.B., Müller, J. Effect of drying on the color of tarragon (*Artemisia dracunculus L*) leaves. *Food and Bioprocess Technology*. **2009** *In Press*
- Baker, C.G.J. ; Khan, A.R.; Ali, Y.I.; Damyar, K. Simulation of plug flow fluidized bed dryers. *Chemical Engineering and Processing* **2006**, 45(8): 641-651
- Courtois, F. Drying of air. *Encyclopedia of Agricultural, Food, and Biological Engineering* **2003**, 1(1); 227-230
- Djaeni, M.; Bartels, P.V; Sanders, J.P.M; Straten, G. van; Boxtel, A.J.B. van. Process integration for food drying with air dehumidified by zeolites. *Drying Technology* **2007a**, 25 (1); 225-239
- Djaeni, M.; Bartels, P.V; Sanders, J.P.M; Straten, G. van; Boxtel, A.J.B. van. Multistage Zeolite Drying for Energy-Efficient Drying. *Drying Technology* **2007b**, 25 (6); 1063-1077
- Djaeni, M.; Bartels, P.; Sanders, J.; Straten, G. van; Boxtel, A.J.B. van. Computational fluid dynamics for multistage adsorption dryer design. *Drying Technology* **2008**, 26 (4); 487-502
- Djaeni, M.; Bartels P.V.; Sanders J.P.M.; van Straten, G.; van Boxtel, A.J.B. Energy Efficiency of Low Temperature Multistage Adsorption Drying. *Journal of Drying Technology* **2009**, 27(4); 555-564
- Gorbach, A.; Stegmaier, M.; Eigenberger, G. Measurement and modeling of water vapor adsorption on zeolite 4A—Equilibria and kinetics. *Adsorption* **2004**, 10; 29-46
- Holmberg, H.; Ahtila, P. Comparison of drying costs in biofuel drying between multistage and single-stage drying. *Journal of Biomass and Bioenergy* **2004**, 26(6): 515-530
- Jenkins, S.A.; Waszkiewicz, S.; Quarini, G.L.; Tierney, M.J. Drying saturated zeolite pellets to assess fluidised bed performance. *Applied Thermal Engineering* **2002**, 22(7); 861-871

- Kim, K.R.; Lee, M.S.; Paek, S.; Yim, S.P.; Ahn, D.H.; Chung, H. Adsorption tests of water vapor on synthetic zeolites for an atmospheric detritiation dryer. *Radiation Physics and Chemistry* **2007**, *76*; 1493-1496
- Krokida, M.K.; Bisharat, G.I. Heat recovery from dryer exhaust air. *Drying Technology* **2004**, *22* (7): 1661-1674
- Mishkin, M., Saguy, I. and Karel, M. Optimization of Nutrient Retention During Processing: Ascorbic Acid in Potato Dehydration. *Journal of Food Science* **1984**, *49*(5): 1262-1266
- Ibrahim, M.; Sopian, K.; Daud, W.R.W. Study of the Drying Kinetics of Lemon Grass. *American Journal of Applied Sciences* **2009**, *6*; 1070-1075
- Nagaya, K.; Li, Y.; Jin, Z.; Fukumuro, M.; Ando, Y.; Akaishi, A. Low-temperature desiccant-based food drying system with air flow and temperature control. *Journal of Food Engineering* **2006**, *75*; 71-77
- Ratti C. Hot air and freeze-drying of high-value foods: a review. *Journal of Food Engineering* **2001**, *49*; 311-319
- Revilla, G.O.; Velázquez, T.G.; Cortéz, S.L.; Cárdenas, S.A. Immersion drying of wheat using Al-PILC, zeolite, clay and sand as particulate media. *Drying Technology* **2006**, *24*, 1033-1038
- Temple, S.J.; van Boxtel, A.J.B.; van Straten, G. Control of fluid bed tea dryers: controller performance under varying operating conditions. *Computers and Electronics in Agriculture* **2000**, *29*(3), 217-231
- Witinantakit, K.; Prachayawarakom, S.; Nathakarakakule, A.; Soponronnarit, S. Paddy drying using adsorption technique: Experiments and simulation. *Drying Technology* **2006**, *24* (5); 609-617
- Zhang, B.G.; Zhou, Y.D.; Ning, W.; Xie, D.B. Experimental study on energy consumption of combined conventional and dehumidification drying. *Drying Technology* **2007**, *25*;471-474